

# Interlayer coupling and superconducting properties of the triple-layer compound $B_{0.6}C_{0.4}(Sr_{0.25}Ba_{0.75})_2Ca_2Cu_3O_9$

Mun-Seog Kim and Sung-Ik Lee

*Department of Physics, Pohang University of Science and Technology, Pohang 790-784, Republic of Korea*

A. Iyo, K. Tokiwa, M. Tokumoto, and H. Ihara

*Electrotechnical Laboratory, Umezono 1-1-4, Tsukuba, Ibaraki 305, Japan*

(Received 24 July 1997; revised manuscript received 21 November 1997)

We report the experimental results on the reversible magnetization of the triple-layer compound  $B_{0.6}C_{0.4}(Sr_{0.25}Ba_{0.75})_2Ca_2Cu_3O_9$  with  $T_c \approx 119$  K. In comparison with  $HgBa_2Ca_2Cu_3O_{8+\delta}$ , which is the same triple-layer compound, this superconductor showed enhanced interlayer coupling due to relatively short interlayer spacing. This feature was reflected by the three-dimensional scaling behavior of the fluctuation-induced magnetization around  $T_c(H)$ . On the other hand, the charge-carrier density calculated from the conventional theories was significantly smaller than the value on  $HgBa_2Ca_2Cu_3O_{8+\delta}$ . The relatively large penetration depth  $\lambda_{ab}(0) = 214$  nm of this superconductor might be due to the small carrier density. We conclude that the competition between enhanced interlayer coupling strength and reduced carrier density make the  $T_c$  of  $B_{0.6}C_{0.4}(Sr_{0.25}Ba_{0.75})_2Ca_2Cu_3O_9$  lower than that of  $HgBa_2Ca_2Cu_3O_{8+\delta}$ . [S0163-1829(98)01314-9]

## I. INTRODUCTION

Since the discovery of superconductivity in layered copper-oxycarbonate  $(Ba_xSr_{1-x})_2Cu_{1+y}O_{2+2y+\delta}(CO_3)_{1-y}$  ( $0.4 \leq x \leq 0.65$ ,  $y \sim 0.1$ ), various oxycarbonate superconductors have been synthesized by a number of groups.<sup>1-4</sup> Especially, Uehara *et al.*<sup>2</sup> reported a homologous series  $(B_xC_{x-1})Sr_n(Ca,Sr)_{n-1}Cu_nO_y$  ( $n = 1, 2, \text{ and } 3$ ). In this family, the double- and triple-layer compounds ( $n = 2$  and  $3$ ) are materials which have superconducting transition temperatures as high as  $\sim 100$  K like Bi-, Tl-, and Hg-based superconductors.

The crystal structure of this series is similar to that of the Hg-based homologous series  $HgBa_2Ca_{n-1}Cu_nO_{2n+2+\delta}$  except for the replacement of Hg by  $CO_3$  and  $BO_3$ . For Hg-based superconductors, the hole concentration in the  $CuO_2$  planes is determined by an interstitial oxygen defect in the  $HgO_\delta$  plane. For the oxycarbonates, the hole-doping level can be controlled systematically by changing the relative content of  $(BO_3)^{3-}$  and  $(CO_3)^{2-}$ . Thus, the substitution of  $(BO_3)^{3-}$  for  $(CO_3)^{2-}$  causes the charge (hole) transfer into the  $CuO_2$  planes.

In comparison with the Hg-based superconductors, the  $c$ -axis lattice parameters of the oxycarbonate series are much reduced. While the parameters with respect to  $n$  are scaled as  $c = 9.5 + 3.2 \times (n - 1)$  Å for the Hg-based superconductors, the parameters of the oxycarbonate series are scaled as  $c = 7.4 + 3.2 \times (n - 1)$  Å. Because a small  $c$ -axis lattice parameter means a small separation between the  $CuO_2$  planes, the interlayer coupling strengths of oxycarbonate superconductors are expected to be strong. It is well known that the interlayer coupling (the interlayer tunneling<sup>5,6</sup> or the interlayer pairing<sup>7,8</sup>) plays an important role in high- $T_c$  superconductivity of the layered materials.<sup>9</sup> Thus, it is very interesting to investigate how the interlayer spacing affects the superconductivity of the oxycarbonate series.

To understand this, we measured the reversible magnetization of the triple-layer compound  $B_{0.6}C_{0.4}(Sr_{0.25}Ba_{0.75})_2Ca_2Cu_3O_9$  (BC-1223) with  $T_c \approx 119$  K. The magnetization was analyzed using the high-field scaling law proposed by Ullah and Dorsey<sup>10</sup> and the Hao and Clem model.<sup>11,12</sup> Here, we concentrate on elucidating the differences between the superconducting properties of BC-1223 and  $HgBa_2Ca_2Cu_3O_{8+\delta}$  (Hg-1223;  $T_c \approx 135$  K). The number of the  $CuO_2$  planes in these compounds is the same. In this study, we may understand why and how the superconductivity changes for these nearly same-structured materials.

## II. EXPERIMENTAL ASPECTS

Details on the sample preparation was given elsewhere.<sup>4</sup> The sample was synthesized from starting powders of  $Ba_2Ca_2Cu_3O_7$ ,  $Sr_2Ca_2Cu_3O_7$ ,  $B_2O_3$ , and  $Ag_2CO_3$ .  $Ag_2CO_3$  was used only for a source of  $CO_3$ . Precursors of  $Ba_2Ca_2Cu_3O_7$  and  $Sr_2Ca_2Cu_3O_7$  were prepared by calcining a well-ground mixture of  $BaCO_3$  (or  $SrCO_3$ ),  $CaCO_3$  and  $CuO$  powders in a flowing oxygen atmosphere. The starting mixtures were sealed in a gold capsule and treated at  $1100^\circ C$  for 3 h under 4.5 GPa with a cubic-anvil-type high-pressure apparatus. The samples were subsequently quenched to room temperature before releasing the pressure. This compound has a tetragonal symmetry ( $p4/mmm$ ) with lattice parameters of  $a = 3.862$  Å and  $c = 14.135$  Å.

The hole-doping state of this sample is not conclusive yet. However, we guess that the negative curvature<sup>4</sup> in the temperature dependence of the normal-state resistivity reflects the under-doped state of the sample. However, because of the considerably high-transition temperature of the sample, we believe that the doping level is not far from the optimal state.

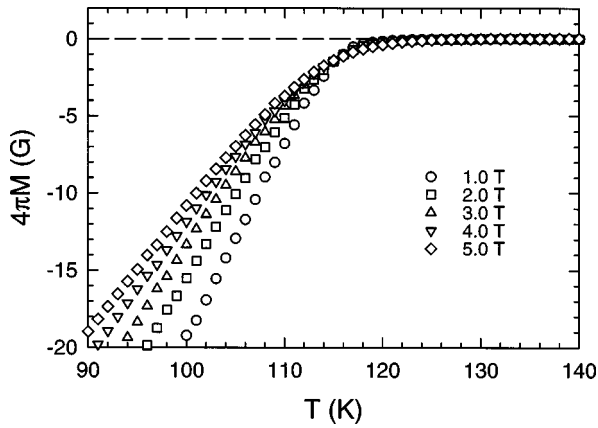


FIG. 1. Temperature dependence of the magnetization  $4\pi M(T)$  in the field range of  $1\text{ T} \leq H \leq 5\text{ T}$  parallel to the  $c$  axis.

To obtain a  $c$ -axis-aligned sample, Farrell's method<sup>13</sup> was employed. The powder of the sample was passed through a  $20\text{ }\mu\text{m}$  sieve to remove possible intergrain coupling, thus the average grain size was expected to be much smaller than  $20\text{ }\mu\text{m}$ . This fine powder was aligned in commercial epoxy (Hardman Inc.) with an external magnetic field of  $7\text{ T}$ . The size of the permanently aligned sample was approximately  $9.5\text{ mm}$  long and  $3\text{ mm}$  in diameter. From the x-ray rocking curve measurement the full width at half maximum of the (006) reflection was estimated to be less than  $2^\circ$ . The low-field dc susceptibility measurement reveals the transition temperature,  $T_c \approx 119\text{ K}$ , the transition width,  $\Delta T_c \approx 7\text{ K}$ , and the superconducting volume fraction,  $V_s \approx 98\%$  of the sample.

The temperature dependence of magnetization was measured in the magnetic-field range of  $1\text{ T} \leq H \leq 5\text{ T}$  using a superconducting quantum interference device magnetometer (MPMS, Quantum Design). Weak temperature-dependent contributions originated from the epoxy and the paramagnetic impurities were appropriately subtracted from the observed values by fitting the magnetization curve at the temperature region of  $200\text{ K} \leq T \leq 250\text{ K}$  by  $C/T + \chi_0$ .

### III. RESULTS AND DISCUSSIONS

Figure 1 shows the temperature dependence of the reversible magnetization for the various external magnetic fields of  $1\text{ T} \leq H \leq 5\text{ T}$  parallel to the  $c$  axis. In this figure an intriguing feature is the existence of the crossing point of the magnetization curves at  $T^* \approx 115\text{ K}$ , previously known clear evidence for the positional fluctuations of vortices, i.e., the vortex fluctuation effect.<sup>14</sup> This effect causes the magnetization curves to deviate from the prediction of the mean-field theories.<sup>15</sup> Thus, quantities such as the upper critical field  $H_{c2}(T)$  and the Ginzburg-Landau (GL) parameter  $\kappa(T)$  evaluated by the application of the Hao and Clem model base on the GL theory show unphysical increase with temperature near the crossing temperature  $T = T^*$ .

Figure 2 shows the GL parameter as a function of temperature, obtained from the Hao and Clem model. The abrupt increase of  $\kappa$  with the temperature near  $T = 105\text{ K}$  ( $\approx 0.9T_c$ ) is clearly demonstrated. As mentioned above, this is due to the influence of the positional fluctuations of vortices.<sup>15,16</sup> However, unlike in the highly anisotropic materials such as

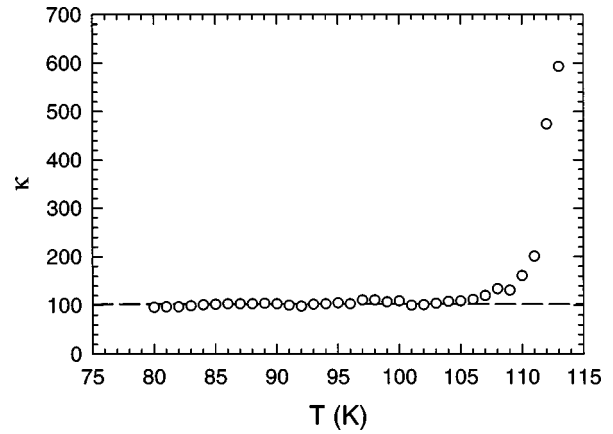


FIG. 2. Temperature dependence of the Ginzburg-Landau parameter  $\kappa(T)$  extracted from the Hao and Clem model. The dashed line represents the average value of  $\kappa(T)$  in the temperature range of  $80\text{ K} \leq T \leq 105\text{ K}$ .

Bi-based superconductors,<sup>15</sup> the temperature region showing the anomalous behavior is significantly narrow ( $T/T_c \geq 0.9$ ), which implies that the vortex fluctuation effect is severe in the limited temperature region near  $T_c$ . This indicates that BC-1223 might be a rather moderately anisotropic superconductor like  $\text{YBa}_2\text{Cu}_3\text{O}_{7-\delta}$  (Ref. 17) and  $\text{YBa}_2\text{Cu}_4\text{O}_8$ ,<sup>18,19</sup> because the vortex fluctuation effect is dominant only for large anisotropic cases.<sup>15</sup>

The anisotropic nature of BC-1223 could be examined from the scaling behavior of the fluctuation-induced magnetization for the high-field region. This scaling behavior depends on the dimensionality of the system. According to Ullah and Dorsey,<sup>10</sup> the magnetization in the critical region shows the scaling behavior as the scaling variable of  $A[T - T_c(H)]/(TH)^n$ , where  $A$  is a field and transition temperature-independent coefficient, and  $n$  is  $2/3$  for a three-dimensional (3D) system and  $1/2$  for a two-dimensional (2D) system. As expected, the magnetization scales excellently on the 3D form. Figure 3 shows the  $4\pi M/(TH)^n$  versus the scaling parameter  $[T - T_c(H)]/(TH)^n$  with  $n = 2/3$ . All data of the different fields are collapsed onto a single curve. The slope  $-dH_{c2}/dT = 1.6\text{ T/K}$  near  $T_c$  was obtained from this scaling analysis.

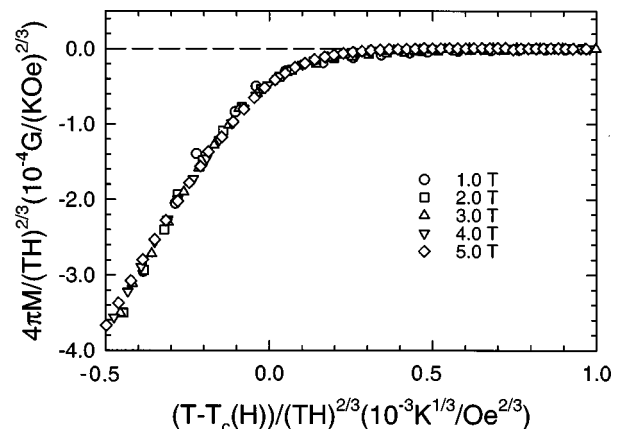


FIG. 3. Three-dimensional scaling of the magnetization around  $T_c(H)$ . From this scaling analysis the slope  $-dH_{c2}/dT = 1.6\text{ T/K}$  near  $T_c$  was obtained.

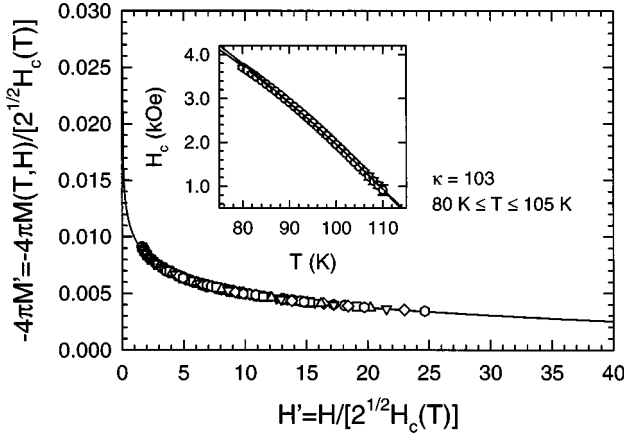


FIG. 4. Magnetization  $-4\pi M' = -4\pi M/\sqrt{2}H_c(T)$  vs external magnetic field  $H' = H/\sqrt{2}H_c(T)$ . The solid line represents the universal curve derived from the Hao and Clem model, assuming  $\kappa = 103$ . Inset: Temperature dependence of the thermodynamic critical field  $H_c(T)$ . The solid and dashed lines represent the BCS temperature dependence and the two-fluid model, respectively.

Although the controversy on the dimensionality of Hg-1223 still exists, it is believed that Hg-1223 is a 2D superconductor<sup>20</sup> with the anisotropic ratio of  $\gamma \approx 30$ . Be aware of the fact that the structure of BC-1223 is nearly same as that of Hg-1223. Thus, it is noticeable that the dimensionality of BC-1223 is 3D. As mentioned in the introduction, the interlayer spacing of BC-1223 is significantly shorter than that of Hg-1223. This feature may cause strong interlayer coupling.

For the temperature region of  $105 \text{ K} \leq T \leq T_c$ , the extra free energy due to the distortions of vortices should be considered to describe the reversible magnetization properly. But the vortex fluctuation effect is less important at the low-temperature region of  $T \leq 105 \text{ K}$ . Thus we conjecture that in this temperature region the system shows the mean-field behavior and the values of  $\kappa(T)$  of Fig. 2 close to the real value. If we take the  $\kappa_{\text{avg}} = 103$  as the average value of  $\kappa(T)$  in the temperature range of  $80 \text{ K} \leq T \leq 105 \text{ K}$ , then  $-4\pi M(H)$  curves could be represented by an universal curve with scaling factor  $\sqrt{2}H_c(T)$ , consistent with the Hao and Clem model. Figure 4 shows  $-4\pi M' = -4\pi M/\sqrt{2}H_c(T)$  versus  $H' = H/\sqrt{2}H_c(T)$  of the experimental data and the theoretical curve.

The inset of Fig. 4 shows the thermodynamic critical field  $H_c$  as a function of the temperature obtained from the Hao and Clem model. The solid and dashed lines represent the BCS result<sup>21</sup> and the two-fluid model<sup>22</sup> for  $H_c(T)$ , respectively. The BCS result (the two-fluid model) yields  $H_c(0) = 0.74 \text{ T}$  (0.69 T) and  $T_c = 118 \text{ K}$ , which correspond to the upper critical field slope  $-(dH_{c2}/dT)_{T_c} = 1.58 \text{ T/K}$ . The value of  $(dH_{c2}/dT)_{T_c}$  is fairly consistent with the high-field scaling result. This slope can be used to estimate the upper critical field at  $T=0$  using the Werthamer, Helfand, and Hohenberg formula.<sup>23</sup> From the formula,  $H_{c2}(0)$  is estimated to be  $136 \text{ T}$  [ $\xi_{ab}(0) = 15.6 \text{ \AA}$ ] assuming the clean limit, and  $130 \text{ T}$  [ $\xi_{ab}(0) = 16.0 \text{ \AA}$ ] assuming the dirty limit. The total error of the above superconducting parameters is estimated to be much less than 10 %.

As shown in Fig. 5, the penetration depth  $\lambda_{ab}(T)$  was

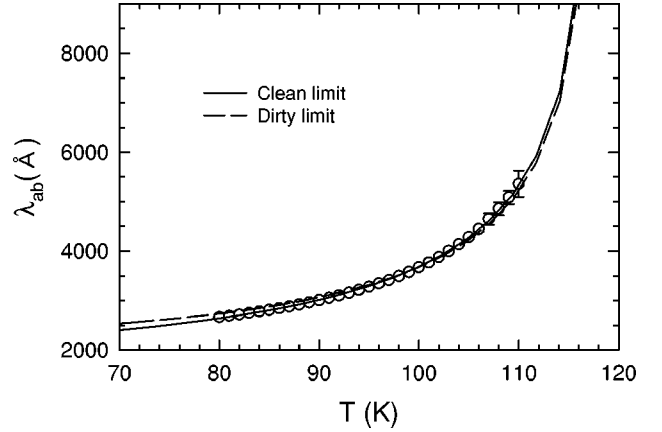


FIG. 5. Temperature dependence of the penetration depth  $\lambda_{ab}(T)$  obtained from the Hao and Clem model. The solid and dashed lines represent the BCS clean and dirty limits, respectively.

evaluated from the relation  $\lambda(T) = \kappa[\phi_0/2\pi H_{c2}(T)]^{1/2}$  where  $\phi_0$  is the flux quantum. The solid and dashed lines represent the BCS clean and dirty limits for  $\lambda(T)$ , respectively. The estimated  $\lambda_{ab}(0)$  is 214 nm for the clean limit, but 237 nm for the dirty limit. These values are considerably larger than  $\lambda_{ab}(0) \leq 170 \text{ nm}$  of Hg-1223,<sup>24-26</sup> which implies that BC-1223 has a small charge-carrier concentration  $n_s$  and/or a large electronic effective mass  $m_{ab}^*$  in comparison with Hg-1223, since the zero-temperature London penetration depth is proportional to  $(m_{ab}^*/n_s)^{1/2}$ .

It is well known that the interlayer coupling strength<sup>5-8</sup> and the charge-carrier concentration within the  $\text{CuO}_2$  planes are responsible in determining the transition temperature of the layered superconductors.<sup>9</sup> The  $T_c$  of BC-1223 is lower than that of Hg-1223, even though BC-1223 shows a strong 3D nature from the enhanced interlayer coupling. Thus we can infer that the relatively low  $T_c$  originates from the relatively small charge-carrier concentration within the  $\text{CuO}_2$  planes.

For the estimation of the carrier concentration  $n_s$ , the following relations<sup>27</sup> based on the GL and the BCS theories can be used:

$$\left(\frac{dH_c}{dT}\right)_{T_c} = -1.7367 \left(\frac{H_c(0)}{T_c}\right) = -4.23\gamma^{1/2}, \quad (1)$$

$$\left(\frac{dH_{c2}}{dT}\right)_{T_c} = -9.55 \times 10^{24} \gamma^2 T_c \left(n_s^{2/3} \frac{S}{S_F}\right)^{-2}, \quad (2)$$

where  $\gamma$  is the Sommerfeld constant,  $S$  is the Fermi-surface area, and  $S_F$  is the Fermi-surface area for a free-electron gas density  $n_s$ . Assuming  $S \approx S_F$ , we obtained  $\gamma = 663 \text{ erg/cm}^3 \text{ K}^2$  and  $n_s = 2.3 \times 10^{21} \text{ cm}^{-3}$  from the values  $H_c(0)$ ,  $T_c$ , and  $(dH_{c2}/dT)_{T_c}$ . These values are much smaller than  $\gamma \approx 1290 \text{ erg/cm}^3 \text{ K}^2$  and  $n_s = 5.5 \times 10^{21} \text{ cm}^{-3}$  for Hg-1223 calculated using the values<sup>24</sup> of  $H_c(0) = 1.17 \text{ T}$ ,  $T_c = 133.5 \text{ K}$ , and  $-(dH_{c2}/dT)_{T_c} = 2.2 \text{ T/K}$ .

#### IV. CONCLUSION

The temperature dependence of the magnetization was measured for the  $c$ -axis oriented

$B_{0.6}C_{0.4}(Sr_{0.25}Ba_{0.75})_2Ca_2Cu_3O_9$  in the field range of  $1\text{ T} \leq H \leq 5\text{ T}$ . The strong interlayer coupling of this material was reflected by the three-dimensional scaling behavior of the fluctuation-induced magnetization and the narrow temperature region of the prominent vortex fluctuations. This result originates from the relatively short interlayer spacing. By the application of the Hao and Clem model, we obtained various superconducting parameters such as the slope  $(dH_{c2}/dT)_{T_c}$  and the in-plane penetration depth  $\lambda_{ab}(0)$ . Especially, the  $\lambda_{ab}(0) = 214\text{ nm}$  is significantly larger than that

of  $HgBa_2Ca_2Cu_3O_{8+\delta}$ . This comparison reveals that the charge-carrier concentration within the  $CuO_2$  planes of  $B_{0.6}C_{0.4}(Sr_{0.25}Ba_{0.75})_2Ca_2Cu_3O_9$  is relatively smaller than that of  $HgBa_2Ca_2Cu_3O_{8+\delta}$ .

#### ACKNOWLEDGMENTS

This work was supported by the Korean Research Foundation, the Korean Ministry of Education, the BSRI of POSTECH, the Korea Science and Engineering Foundation (Contract No. 95-0702-03-01-3 and 961-0207-042-2).

- 
- <sup>1</sup>M. Uehara, H. Nakata, and J. Akimitsu, *Physica C* **216**, 456 (1993).
- <sup>2</sup>M. Uehara, M. Uoshima, S. Ishiyama, H. Nakata, J. Akimitsu, Y. Matsui, T. Arima, Y. Tokura, and N. Mori, *Physica C* **229**, 310 (1994).
- <sup>3</sup>J. Akimitsu, M. Sato, H. Takahashi, and N. Mori, *Physica C* **271**, 79 (1996).
- <sup>4</sup>A. Iyo, K. Tokiwa, N. Terada, M. Tokumoto, and H. Ihara, *Czech. J. Phys.* **46**, 1481 (1996).
- <sup>5</sup>J. M. Wheatley, T. C. Hsu, and P. W. Anderson, *Phys. Rev. B* **37**, 5897 (1988).
- <sup>6</sup>S. Chakravarty, A. Sudbø, P. W. Anderson, and S. Strong, *Science* **261**, 337 (1993).
- <sup>7</sup>Zlatko Tešanović, *Phys. Rev. B* **36**, 2364 (1987).
- <sup>8</sup>Z. Ye, H. Umezawa, and R. Teshima, *Phys. Rev. B* **44**, 351 (1991).
- <sup>9</sup>S. L. Cooper and K. E. Gray, in *Physical Properties of High Temperature Superconductors IV*, edited by D. M. Ginsberg (World Scientific, Singapore, 1994), p. 61.
- <sup>10</sup>Salman Ullah and Alan T. Dorsey, *Phys. Rev. Lett.* **65**, 2066 (1990).
- <sup>11</sup>Zhidong Hao and John R. Clem, *Phys. Rev. Lett.* **67**, 2371 (1991).
- <sup>12</sup>Zhidong Hao, John R. Clem, M. W. McElfresh, L. Civale, A. P. Malozemoff, and F. Holtzberg, *Phys. Rev. B* **43**, 2844 (1991).
- <sup>13</sup>D. E. Farrell, B. S. Chandrasekhar, M. R. DeGuire, M. M. Fang, V. G. Kogan, J. R. Clem, and D. K. Finnemore, *Phys. Rev. B* **36**, 4025 (1987).
- <sup>14</sup>L. N. Bulaevskii, M. Ledvij, and V. G. Kogan, *Phys. Rev. Lett.* **68**, 3773 (1992).
- <sup>15</sup>V. G. Kogan, M. Ledvij, A. Yu. Simonov, J. H. Cho, and D. C. Johnston, *Phys. Rev. Lett.* **70**, 1870 (1993).
- <sup>16</sup>Mun-Seog Kim, Sung-Ik Lee, and W. C. Lee, *Chin. J. Phys.* **34**, 414 (1996).
- <sup>17</sup>U. Welp, S. Fleshler, W. K. Kwok, R. A. Klemm, V. M. Vinokur, J. Downey, B. Veal, and G. W. Crabtree, *Phys. Rev. Lett.* **67**, 3180 (1991).
- <sup>18</sup>Junghyun Sok, Ming Xu, Wei Chen, B. J. Suh, J. Gohng, D. K. Finnemore, M. J. Kramer, L. A. Schwatzkopf, and B. Dabrowski, *Phys. Rev. B* **51**, 6035 (1995).
- <sup>19</sup>Mun-Seog Kim, Wan-Seon Kim, Sung-IK Lee, Seong-Cho Yu, Jin-Tae Kim, and B. Dabrowski, *J. Appl. Phys.* **81**, 4231 (1997).
- <sup>20</sup>C. Panagopoulos, J. R. Cooper, G. B. Peacock, I. Gameson, P. P. Edwards, W. Schmidbauer, and J. W. Hodby, *Phys. Rev. B* **53**, 2999 (1996).
- <sup>21</sup>J. R. Clem, *Ann. Phys. (N.Y.)* **40**, 286 (1966).
- <sup>22</sup>C. J. Gorter and H. B. G. Casimir, *Physica (Amsterdam)* **1**, 306 (1934).
- <sup>23</sup>N. R. Werthamer, E. Helfand, and P. C. Hohenberg, *Phys. Rev.* **147**, 295 (1966).
- <sup>24</sup>J. R. Thompson, J. G. Ossandon, D. K. Christen, M. Paranthaman, E. D. Specht, and Y. C. Kim, *Phys. Rev. B* **54**, 7505 (1996).
- <sup>25</sup>Y. C. Kim, J. R. Thompson, J. G. Ossandon, D. K. Christen, and M. Paranthaman, *Phys. Rev. B* **51**, 11 767 (1995).
- <sup>26</sup>R. Puźniak, R. Usami, K. Isawa, and H. Yamauchi, *Phys. Rev. B* **52**, 3756 (1995).
- <sup>27</sup>T. P. Orlando, Jr., E. J. McNiff, S. Foner, and M. R. Beasley, *Phys. Rev. B* **19**, 4545 (1979).